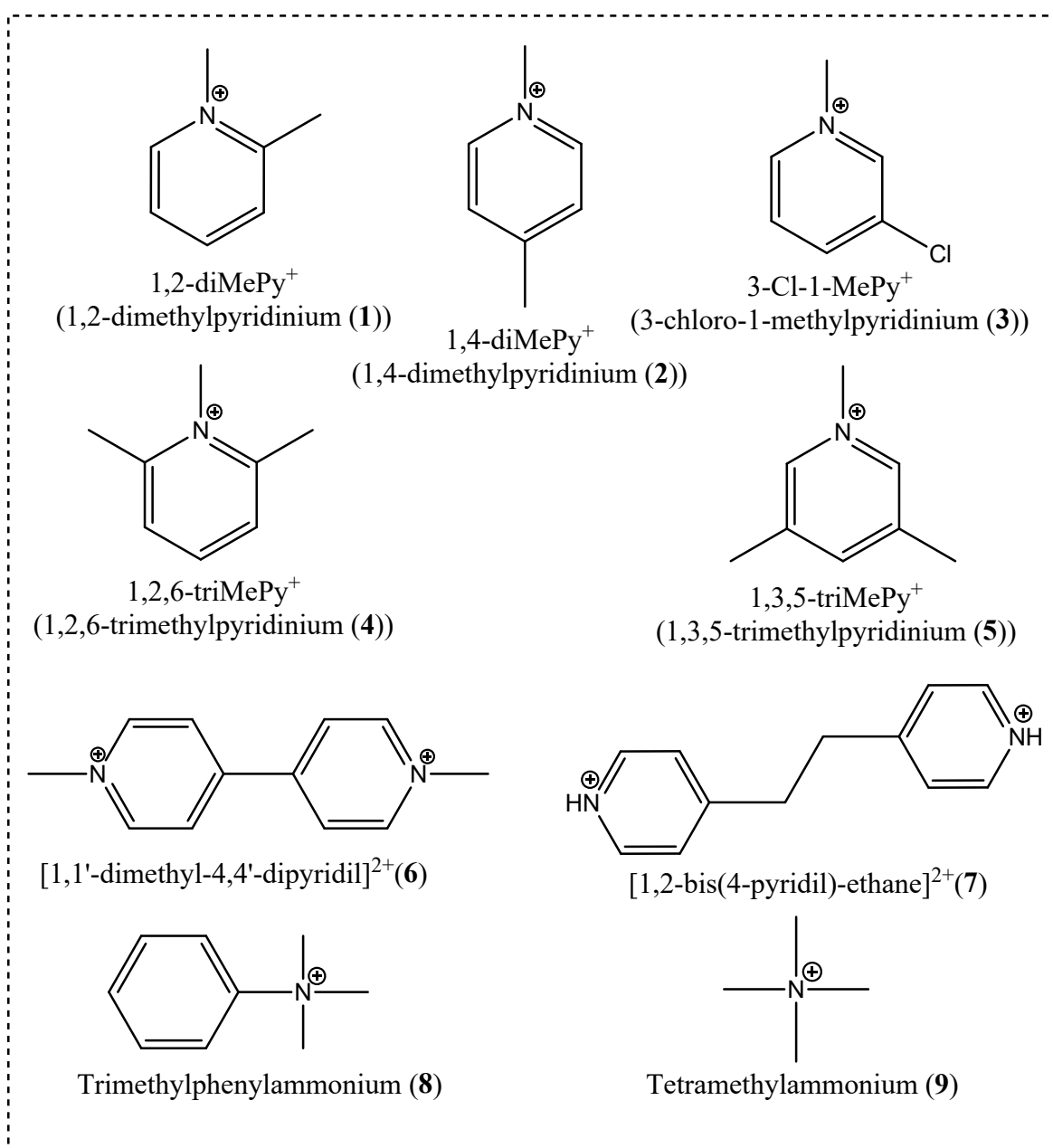
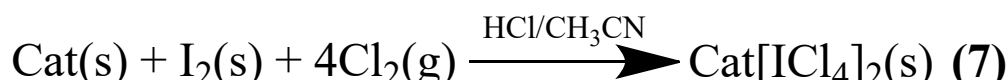
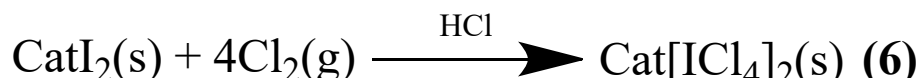


Supplementary Information

**Halogen bonding in chloroiodates(III)**

Nikita A. Korobeynikov, Andrey N. Usoltsev, Maxim N. Sokolov, Alexander S. Novikov, Taisiya S. Sukhikh and Sergey A. Adonin



**Scheme S1.** Reaction schematics and cations utilized in this work.

### Synthesis of 1–5

0.20 mmol of corresponding pyridine iodide (47 mg in **1** and **2**, 51 mg in **3**, 50 mg in **4** and **5**) were dissolved in 7 mL of concentrated hydrochloric acid with heating to 60 °C. Then gaseous chlorine was bubbled through the solutions until all reactants were dissolved. Resulting mixtures were slowly cooled to room temperature. Within 24 hours, yellow crystalline precipitates formed in all experiments.

### Synthesis of 6

44 mg (0.10 mmol) of 1,1'-dimethyl-4,4'-bipyridine diiodide were dissolved in 6 mL of concentrated hydrochloric acid with to 60 °C. Then gaseous chlorine was bubbled through the solution until all reactants were dissolved. Resulting mixture was slowly cooled to room temperature. Within 24 hours, yellow crystals formed.

### Synthesis of 7

37 mg (0.20 mmol) of 1,2-bis(4-pyridil)ethane were dissolved in 5 mL of concentrated hydrochloric acid upon heating up to 60 °C. Then 51 mg (0.20 mmol) of I<sub>2</sub> were added into solution followed by addition of 2 mL of CH<sub>3</sub>CN. Gaseous chlorine was bubbled through the mixture until all iodine was oxidized. Resulting solution was cooled to room temperature. Upon slow evaporation of solvents (CH<sub>3</sub>CN at most) within 24 hours yellow crystals formed.

### Synthesis of 8

53 mg (0.20 mmol) of trimethylethylammonium iodide were dissolved in 6 mL of concentrated hydrochloric acid upon heating to 60 °C. Then gaseous chlorine was bubbled through the solution until all reactants were dissolved. Mixture was slowly cooled to room temperature. After 6 hours, yellow crystals formed.

### Synthesis of 9

44 mg (0.22 mmol) of tetramethylammonium iodide were dissolved in 5 mL of concentrated hydrochloric acid upon heating to 60 °C. Then gaseous chlorine was bubbled through the solution until all reactants were dissolved. Mixture was slowly cooled to room temperature. After 6 hours, yellow crystals formed.

**Table S1.** Elemental analysis data and yields for **1–9**.

Compound	C, H, N, calculated/found, %	Yield, %
<b>1</b>	22.4, 2.7, 3.7/22.1, 2.6, 3.6	86
<b>2</b>	22.4, 2.7, 3.7/22.4, 2.5, 3.7	82
<b>3</b>	18.2, 1.8, 3.5/18.0, 1.7, 3.5	-
<b>4</b>	-	-
<b>5</b>	-	-
<b>6</b>	20.0, 2.0, 3.9/20.1, 2.0, 3.8	78

<b>7</b>	–	–
<b>8</b>	26.8, 3.5, 3.5/26.9, 3.6, 3.5	80
<b>9</b>	–	–

The single crystal X-ray diffraction data for **2–7** were collected with a Bruker D8 Venture diffractometer with a CMOS PHOTON III detector and  $\text{I}\mu\text{S}$  3.0 source ( $\text{Mo K}\alpha$  radiation,  $\lambda = 0.71073 \text{ \AA}$ ,  $\phi$ - and  $\omega$ -scans). Data reduction was performed routinely via Apex3 suite (*Apex3, SADABS 2016/2; Publisher: Bruker AXS Inc., Madison, WI, USA, 2017.*). The data for **1** and **8–9** were collected with an Agilent Xcalibur diffractometer equipped with an area AtlasS2 detector (graphite monochromator,  $\lambda(\text{MoK}\alpha) = 0.71073 \text{ \AA}$ ,  $\omega$ -scans). Data reduction was performed routinely via the CrysAlisPro program package. The crystal structures were solved by SHELXT and refined by the full-matrix least squares technique (SHELXL 2017/1) with Olex2 GUI (2009). Atomic displacements for non-hydrogen atoms were refined in harmonic anisotropic approximation. Hydrogen atoms were refined in the geometrically calculated positions. The structures of **1–9** were deposited to the Cambridge Crystallographic Data Centre (CCDC), No. 2257393-2257401. Details are given in Tables S2-S3.

**Table S2.** Crystal data and structure refinement for compounds **1–5**.

Identification code	<b>1</b>	<b>2</b>	<b>3</b>	<b>4</b>	<b>5</b>
CCDC number	2257393	2257394	2257395	2257396	2257397
Empirical formula	$\text{C}_7\text{H}_{10}\text{ICl}_4\text{N}$	$\text{C}_7\text{H}_{10}\text{ICl}_4\text{N}$	$\text{C}_6\text{H}_7\text{ICl}_4\text{N}$	$\text{C}_8\text{H}_{12}\text{ICl}_4\text{N}$	$\text{C}_8\text{H}_{12}\text{ICl}_4\text{N}$
Formula weight	376.86	376.86	397.28	390.89	390.89
Temperature/K	140	150	150	150	150
Space group	$P2_1/c$	$P2_1/c$	$P2_1$	$C2/c$	$P2_1/c$
$a/\text{\AA}$	8.3175(7)	4.3707(3)	8.2044(2)	17.4476(6)	11.3598(15)
$b/\text{\AA}$	9.8500(5)	11.8303(9)	9.6553(3)	9.9715(4)	8.5116(11)
$c/\text{\AA}$	7.6668(5)	11.8442(10)	8.2874(2)	7.8504(3)	15.140(2)
$\alpha/^\circ$	90	90	90	90	90
$\beta/^\circ$	101.728(7)	92.985(3)	105.887(1)	102.600(1)	110.486(4)
$\gamma/^\circ$	90	90	90	90	90
Volume/ $\text{\AA}^3$	615.01(8)	611.59(8)	631.42 (3)	1332.91(9)	1371.3(3)
Z	2	2	2	4	4
$D_{\text{calc}}/\text{g/cm}^3$	2.035	2.046	2.090	1.948	1.893
$\mu/\text{mm}^{-1}$	3.43	3.45	3.55	3.17	3.08
F(000)	360	360	376	752	752
Tmin, Tmax	0.726, 1.000	0.628, 0.746	0.683, 0.746	0.679, 0.747	0.574, 0.745
2 $\Theta$ range for data collection/ $^\circ$	5.002 to 58.054	4.870 to 59.160	5.110 to 61.042	4.734 to 67.744	3.828 to 52.822
Index ranges	$-8 \leq h \leq 11, -9 \leq k \leq 13, -9 \leq l \leq 9$	$-6 \leq h \leq 5, -16 \leq k \leq 12, -15 \leq l \leq 16$	$-11 \leq h \leq 11, -13 \leq k \leq 13, -11 \leq l \leq 11$	$-26 \leq h \leq 26, -15 \leq k \leq 15, -11 \leq l \leq 10$	$-14 \leq h \leq 14, -10 \leq k \leq 10, -18 \leq l \leq 18$
$R_{\text{int}}$	0.049	0.0317	0.0316	0.0305	0.0590
No. of measured, independent and observed [ $I > 2\sigma(I)$ ]	2679/1360/1043	6479/1712/1479	28732/3847/3782	13777/2315/2021	13909/2811/2334

reflections					
Data/restraints/parameters	1360/18/99	1712/0/62	3847/1/120	2315/0/77	2811/0/131
Goodness-of-fit on $F^2$	1.045	1.040	1.052	1.058	1.031
Final R indices [ $ I  >= 2\sigma(I)$ ]	$R_1 = 0.0392$ , $wR_2 = 0.0905$	$R_1 = 0.0191$ , $wR_2 = 0.0415$	$R_1 = 0.0145$ , $wR_2 = 0.0336$	$R_1 = 0.0166$ , $wR_2 = 0.0351$	$R_1 = 0.0406$ , $wR_2 = 0.0966$
R indices [all data]	0.0557	0.0242	0.0150	0.0220	0.0517
$(\sin \theta/\lambda)_{\max} (\text{\AA}^{-1})$	0.683	0.695	0.715	0.774	0.626
Largest diff. peak/hole/e/ $\text{\AA}^3$	1.25/-1.40	0.35/-0.48	0.38/-0.37	0.42/-0.32	1.39/-1.21

**Table S3.** Crystal data and structure refinement for compounds **6-9**.

Identification code	<b>6</b>	<b>7</b>	<b>8</b>	<b>9</b>
CCDC number	2257398	2257399	2257400	2257401
Empirical formula	$C_{12}H_{14}I_2Cl_8N_2$	$C_{12}H_{14}ICl_5N_2$	$C_9H_{14}ICl_4N$	$C_4H_{12}ICl_4N$
Formula weight	723.65	490.40	404.91	342.85
Temperature/K	150	150	140	140
Space group	$P4_2bc$	$P-1$	$P2_1/n$	$P3_2$
a/ $\text{\AA}$	11.5876(8)	7.4887(5)	8.4156(4)	16.4343(5)
b/ $\text{\AA}$	11.5876(8)	7.6756(5)	16.0769(6)	16.4343(5)
c/ $\text{\AA}$	16.4371(15)	8.0494(5)	10.9381(4)	11.4451(4)
$\alpha/^\circ$	90	93.199(2)	90	90
$\beta/^\circ$	90	110.363(2)	103.705(4)	90
$\gamma/^\circ$	90	95.058(3)	90	120
Volume/ $\text{\AA}^3$	2207.0(4)	430.22(5)	1437.75(10)	2677.02(19)
Z	4	1	4	9
$D_{\text{calc}} \text{g/cm}^3$	2.178	1.893	1.871	1.914
$\mu/\text{mm}^{-1}$	3.82	2.63	2.94	3.54
F(000)	1368	238	784	1476
Tmin, Tmax	0.616, 0.746	0.643, 0.746	0.984, 1.000	0.966, 1.000
2 $\Theta$ range for data collection/ $^\circ$	4.956 to 63.086	5.352 to 59.158	4.594 to 57.568	3.558 to 57.802
Index ranges	-17 $\leq h \leq 10$ , -17 $\leq k \leq 15$ , -23 $\leq l \leq 24$	-9 $\leq h \leq 10$ , -10 $\leq k \leq 10$ , -11 $\leq l \leq 10$	-10 $\leq h \leq 9$ , -21 $\leq k \leq 14$ , -14 $\leq l \leq 11$	-20 $\leq h \leq 20$ , -21 $\leq k \leq 13$ , -14 $\leq l \leq 13$
$R_{\text{int}}$	0.0608	0.0258	0.0259	0.0244
No. of measured, independent and observed reflections [ $ I  > 2\sigma(I)$ ]	23479/3676/3154	5544/2276/2207	6822/3177/2744	8457/6215/5776
Data/restraints/parameters	3676/1/110	2276/0/94	3177/0/140	6215/5/268
Goodness-of-fit on $F^2$	1.027	1.079	1.042	1.017
Final R indices [ $ I  >= 2\sigma(I)$ ]	$R_1 = 0.0300$ , $wR_2 = 0.0525$	$R_1 = 0.0282$ , $wR_2 = 0.0619$	$R_1 = 0.0281$ , $wR_2 = 0.0430$	$R_1 = 0.0351$ , $wR_2 = 0.0606$
R indices [all data]	0.0398	0.0293	0.0366	0.0396
$(\sin \theta/\lambda)_{\max} (\text{\AA}^{-1})$	0.736	0.695	0.677	0.680
Largest diff. peak/hole/e/ $\text{\AA}^3$	0.39/-0.53	1.40/-0.44	0.58/-0.64	0.77/-0.60

**Powder X-ray diffraction (PXRD)** data for polycrystalline samples of **1–9** were collected with Shimadzu XRD-7000 diffractometer in the Bragg—Brentano geometry ( $\text{CuK}_\alpha$  radiation, Ni–filter) and Bruker Advance powder diffractometer with an energy discriminating Eiger XE T detector ( $\text{CuK}_\alpha$  radiation). The samples were slightly ground with hexane in an agate mortar, and the resulting suspensions were deposited on the polished side of a standard sample holder, and a smooth thin layer being formed after drying. The diffraction patterns of **1–2, 6, 8** agree well with those simulated from the single crystal XRD data.

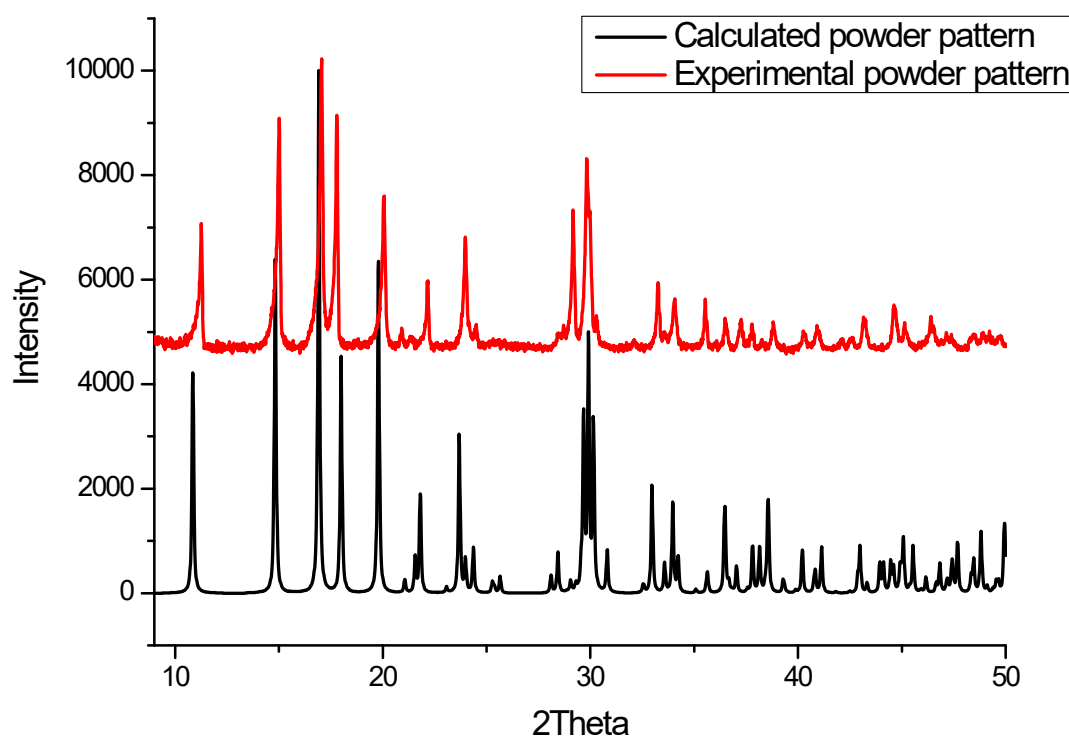


**Figure S1.** Calculated (black) and experimental (red) PXRD patterns of **1**.

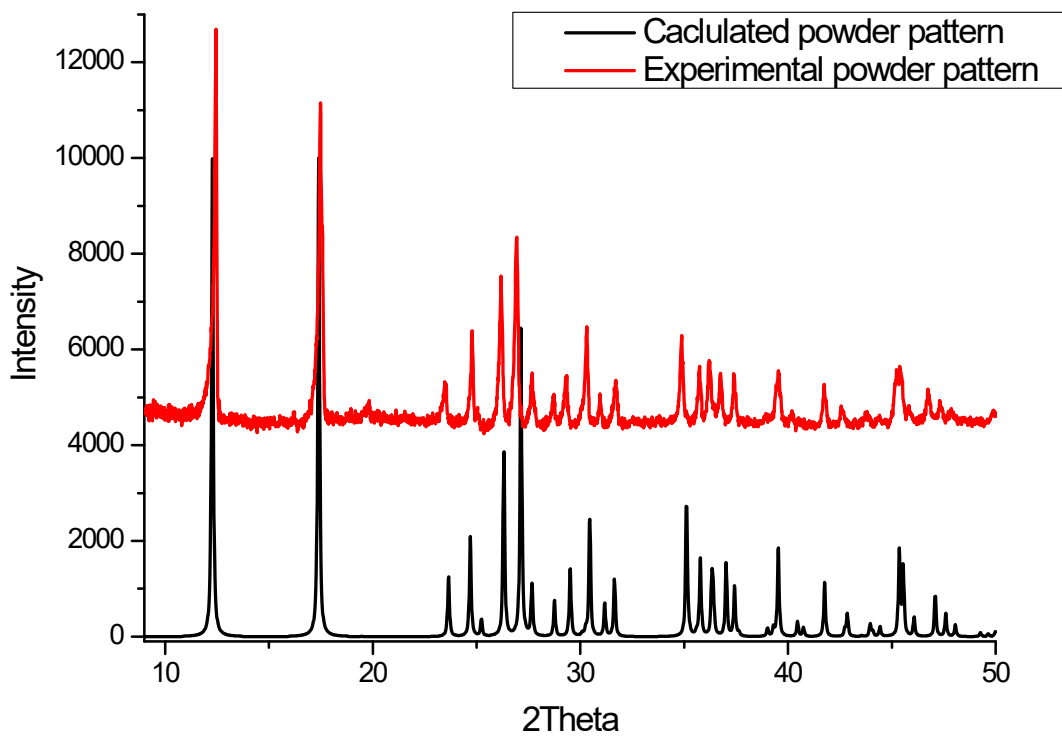


**Figure S2.** Calculated (black) and experimental (red) PXRD patterns of **2**.

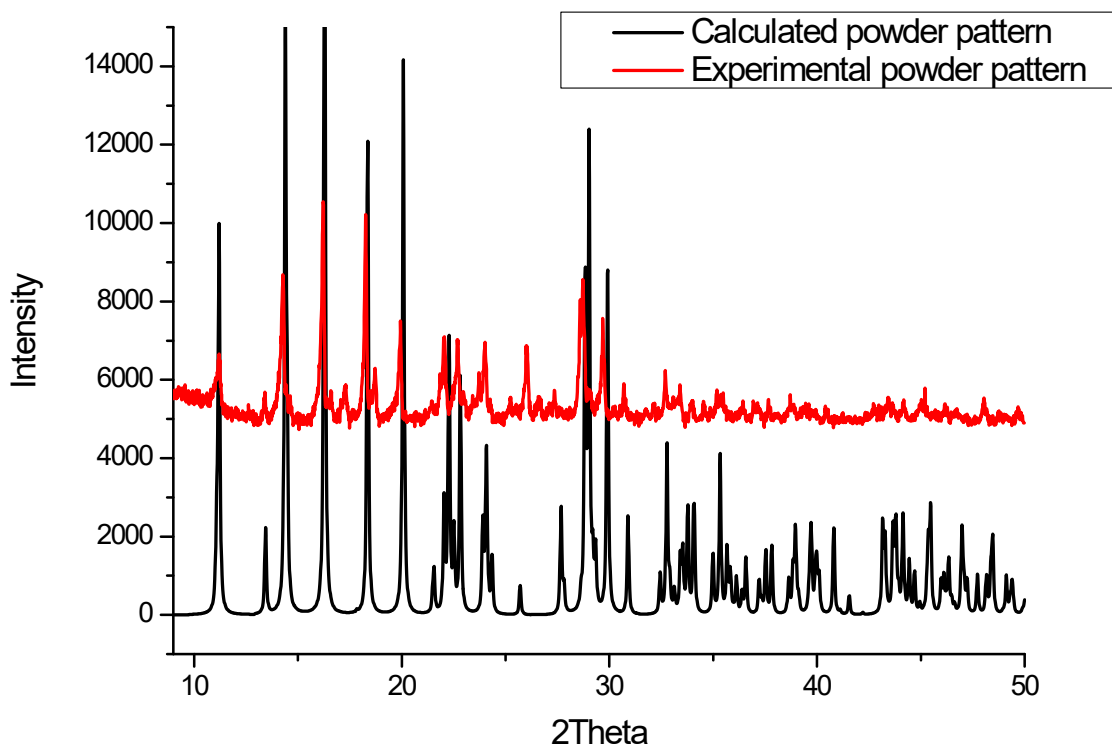


**Figure S3.** Calculated (black) and experimental (red) PXRD patterns of **3**.

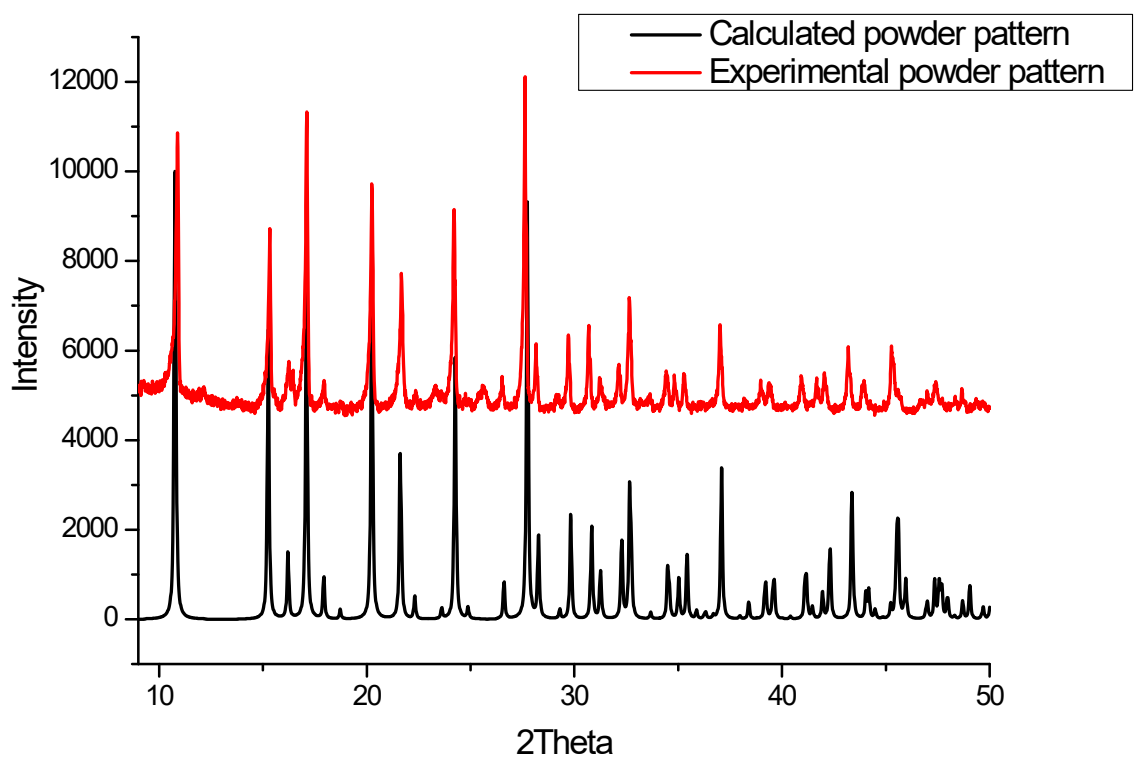


**Figure S4.** Calculated (black) and experimental (red) PXRD patterns of **6**.

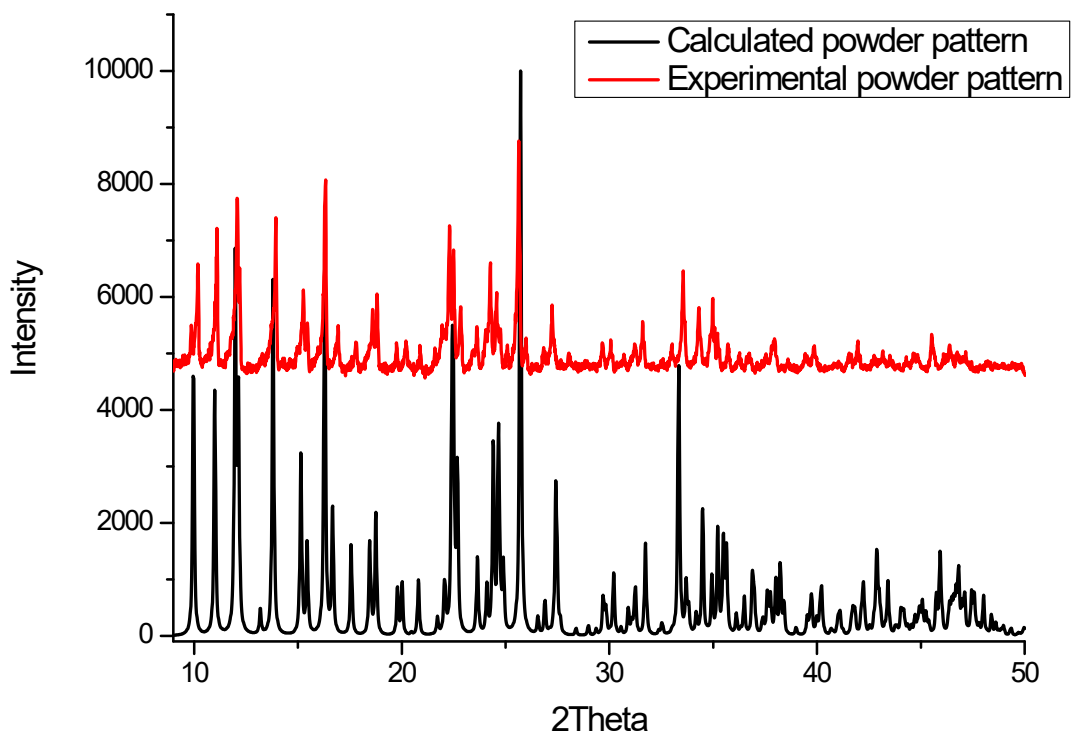


**Figure S5.** Calculated (black) and experimental (red) PXRD patterns of **8**.

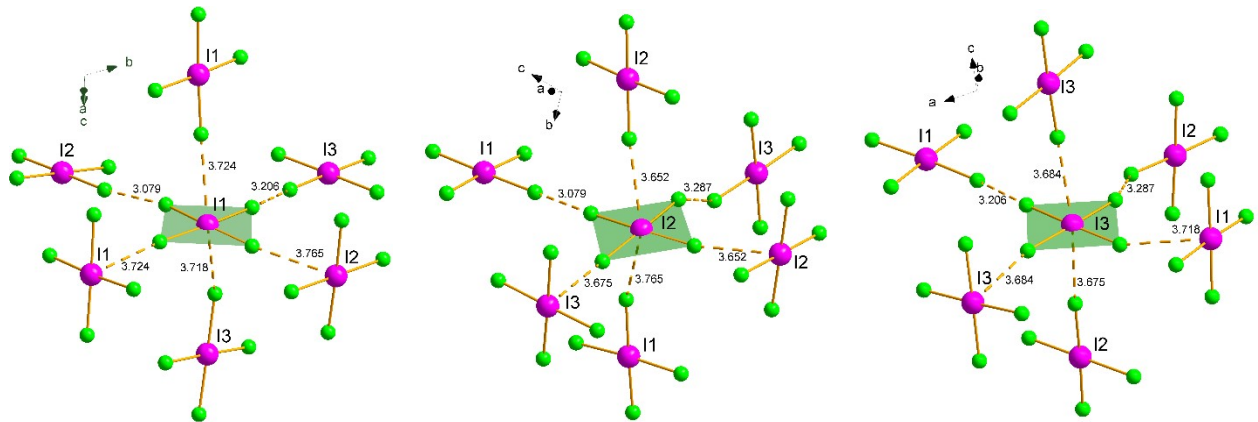


**Figure S6.** Halogen bonding between each of three crystallographically independent  $\text{ICl}_4^-$  anions in compound **9**.

**Table S4.** Halogen bond angles (deg.) between the anions in compound **9**

	I(1)Cl <sub>4</sub>	I(2)Cl <sub>4</sub>	I(3)Cl <sub>4</sub>
I—Cl···I	174.9; 161.2	167.2; 177.1	169.0; 150.8
I—Cl···Cl	168.8; 161.5	170.9; 146.6	169.2; 146.0
I···Cl—I	174.9; 150.8	167.2; 161.2	177.1; 169.0

**Table S5.** Values of the density of all electrons –  $\rho(\mathbf{r})$ , Laplacian of electron density –  $\nabla^2\rho(\mathbf{r})$  and appropriate  $\lambda_2$  eigenvalues, energy density –  $H_b$ , electron localization function – ELF, potential energy density –  $V(\mathbf{r})$ , and Lagrangian kinetic energy –  $G(\mathbf{r})$  (a.u.) at the bond critical points (3, –1), corresponding to intermolecular interactions Cl···Cl and Cl···I in the X-ray structures **1–9**, and estimated strength for these interactions  $E_{\text{int}}$  (kcal/mol).

Model structure*	$\rho(\mathbf{r})$	$\nabla^2\rho(\mathbf{r})$	$\lambda_2$	$H_b$	ELF	$V(\mathbf{r})$	$G(\mathbf{r})$	$E_{\text{int}}^{**}$
<b>1</b>								
Cl···Cl 3.563 Å	0.006	0.020	-0.006	0.001	0.020	-0.003	0.004	0.9
Cl···I 3.755 Å	0.007	0.024	-0.007	0.001	0.018	-0.004	0.005	1.2
<b>2</b>								
Cl···Cl 3.998 Å	0.003	0.008	-0.003	0.001	0.009	-0.001	0.002	0.3
Cl···Cl 3.973 Å	0.004	0.011	-0.004	0.000	0.013	-0.002	0.002	0.6
Cl···I 4.119 Å	0.004	0.014	-0.004	0.001	0.008	-0.002	0.003	0.6
<b>3</b>								
Cl···Cl 3.292 Å	0.010	0.035	-0.010	0.002	0.031	-0.005	0.007	1.5
Cl···Cl 3.652 Å	0.006	0.017	-0.006	0.001	0.020	-0.003	0.004	0.9
Cl···I 3.679 Å	0.008	0.029	-0.008	0.001	0.022	-0.005	0.006	1.5
<b>4</b>								
Cl···Cl 4.074 Å	0.003	0.009	-0.003	0.001	0.008	-0.001	0.002	0.3
Cl···I 3.861 Å	0.005	0.020	-0.005	0.001	0.014	-0.003	0.004	0.9
<b>5</b>								
Cl···Cl 3.887 Å	0.004	0.013	-0.004	0.001	0.015	-0.002	0.003	0.6
Cl···I 3.943 Å	0.005	0.019	-0.005	0.001	0.013	-0.003	0.004	0.9
Cl···I 4.084 Å	0.004	0.015	-0.004	0.001	0.008	-0.002	0.003	0.6
<b>6</b>								
Cl···Cl 3.330 Å	0.009	0.030	-0.009	0.001	0.027	-0.005	0.006	1.5
<b>7</b>								
Cl···Cl 3.579 Å	0.006	0.020	-0.006	0.001	0.021	-0.003	0.004	0.9
Cl···I 3.838 Å	0.007	0.024	-0.007	0.001	0.023	-0.004	0.005	1.2

8								
Cl···Cl 3.491 Å	0.006	0.022	-0.006	0.001	0.021	-0.003	0.004	0.9
Cl···I 3.963 Å	0.005	0.019	-0.005	0.001	0.014	-0.003	0.004	0.9
9								
Cl12···Cl24 3.802 Å	0.005	0.014	-0.005	0.001	0.015	-0.002	0.003	0.6
Cl12···I21 3.718 Å	0.008	0.027	-0.008	0.002	0.022	-0.004	0.006	1.2
Cl15···I16 3.684 Å	0.008	0.028	-0.008	0.002	0.022	-0.004	0.006	1.2
Cl14···Cl4 3.206 Å	0.011	0.040	-0.011	0.001	0.035	-0.007	0.008	2.2
Cl18···Cl9 3.287 Å	0.010	0.036	-0.010	0.001	0.034	-0.006	0.007	1.8
Cl8···Cl3 3.079 Å	0.014	0.050	-0.014	0.002	0.042	-0.009	0.011	2.8
Cl2···I26 3.766 Å	0.007	0.025	-0.007	0.001	0.020	-0.004	0.005	1.2
Cl2···Cl28 3.810 Å	0.005	0.014	-0.005	0.001	0.015	-0.002	0.003	0.6
Cl7···I41 3.652 Å	0.009	0.030	-0.009	0.001	0.026	-0.005	0.006	1.5
Cl5···I31 3.724 Å	0.007	0.027	-0.007	0.001	0.021	-0.004	0.005	1.2
Cl10···I36 3.675 Å	0.008	0.029	-0.008	0.001	0.024	-0.005	0.006	1.5

\* The Bondi's (shortest) van der Waals radii for chlorine and iodine atoms are 1.75 and 1.98 Å, respectively [J. Phys. Chem. 1966, 70, 3006.].

\*\*  $E_{\text{int}} \approx 0.49(-V(r))$  (this empirical correlation between the interaction energy and the potential energy density of electrons at the bond critical points (3, -1) was specifically developed for noncovalent interactions involving chlorine atoms) [Russ. Chem. Rev. 2014, 83, 1181.].

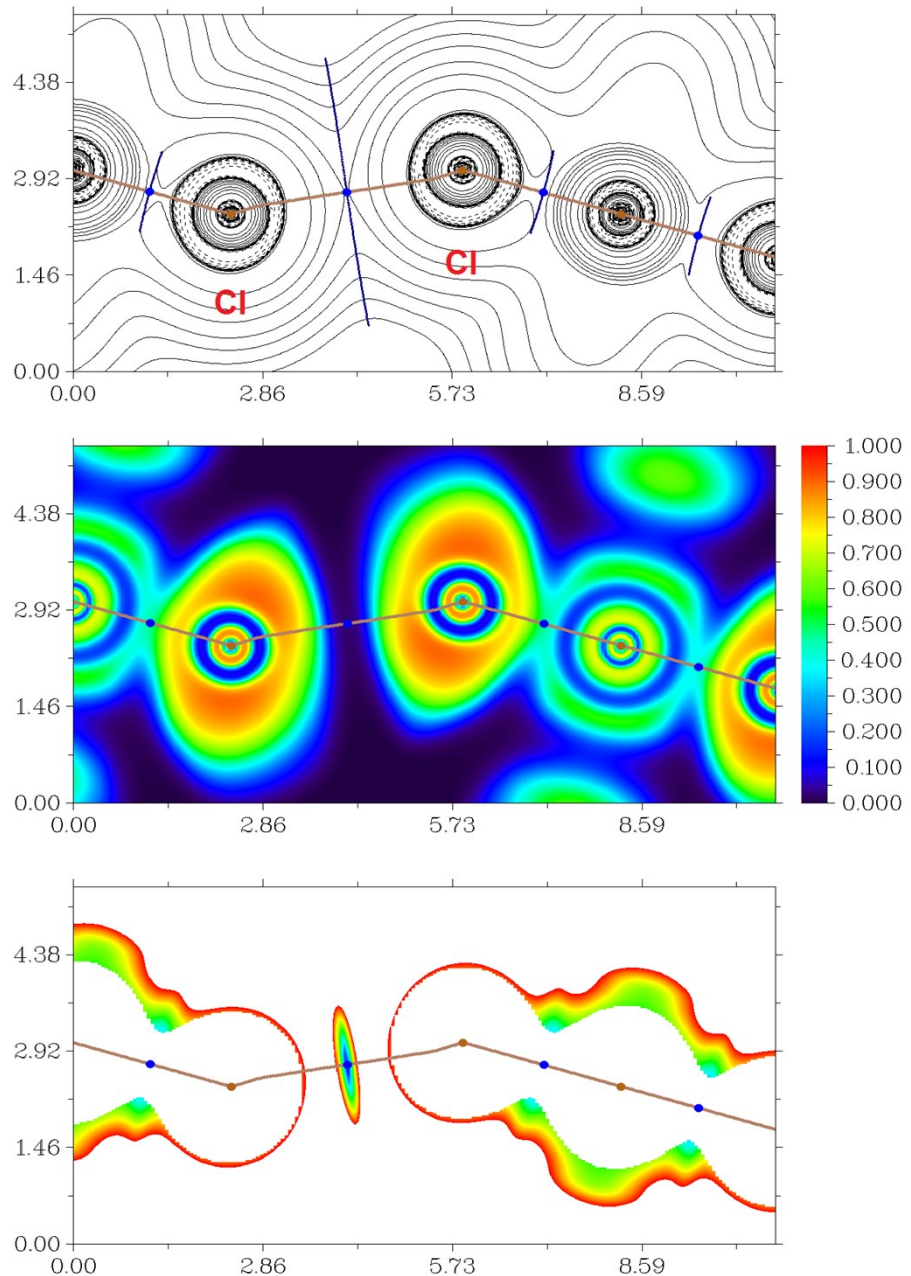


**Figure S7.** Contour line diagram of the Laplacian of electron density distribution  $\nabla^2\rho(\mathbf{r})$ , bond paths, and selected zero-flux surfaces (top), visualization of electron localization function (ELF, center) and reduced density gradient (RDG, bottom) analyses for intermolecular interactions  $\text{Cl}\cdots\text{Cl}$  in **1**. Bond critical points  $(3, -1)$  are shown in blue, nuclear critical points  $(3, -3)$  – in pale brown, bond paths are shown as pale brown lines, length units – Å, and the color scale for the ELF and RDG maps is presented in a.u.

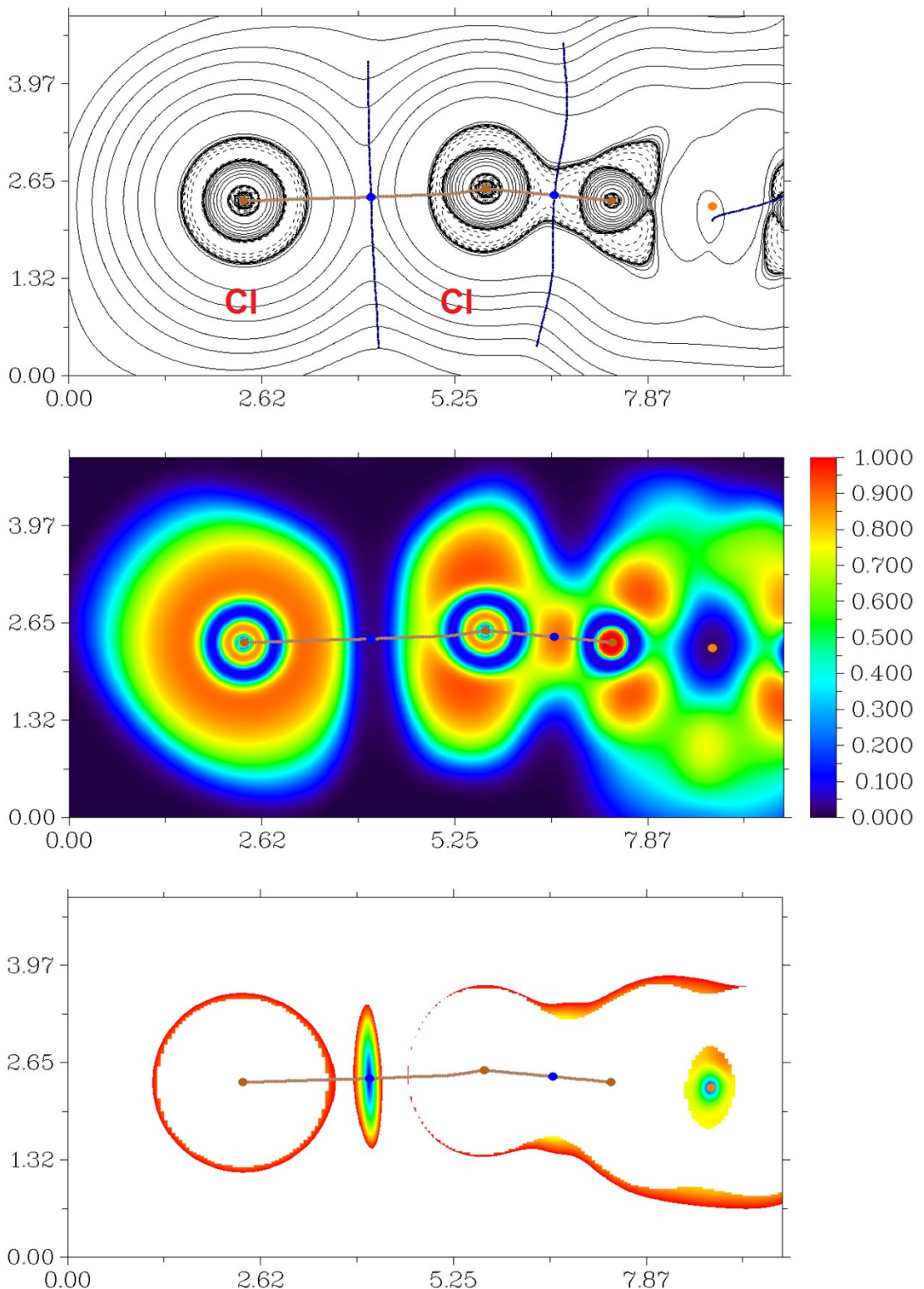


**Figure S8.** Contour line diagram of the Laplacian of electron density distribution  $\nabla^2\rho(\mathbf{r})$ , bond paths, and selected zero-flux surfaces (top), visualization of electron localization function (ELF, center) and reduced density gradient (RDG, bottom) analyses for intermolecular interactions  $\text{Cl}\cdots\text{Cl}$  (3.292 Å) in **3**. Bond critical points (3, -1) are shown in blue, nuclear critical points (3, -3) – in pale brown, ring critical points (3, +1) – in orange, bond paths are shown as pale brown lines, length units – Å, and the color scale for the ELF and RDG maps is presented in a.u.

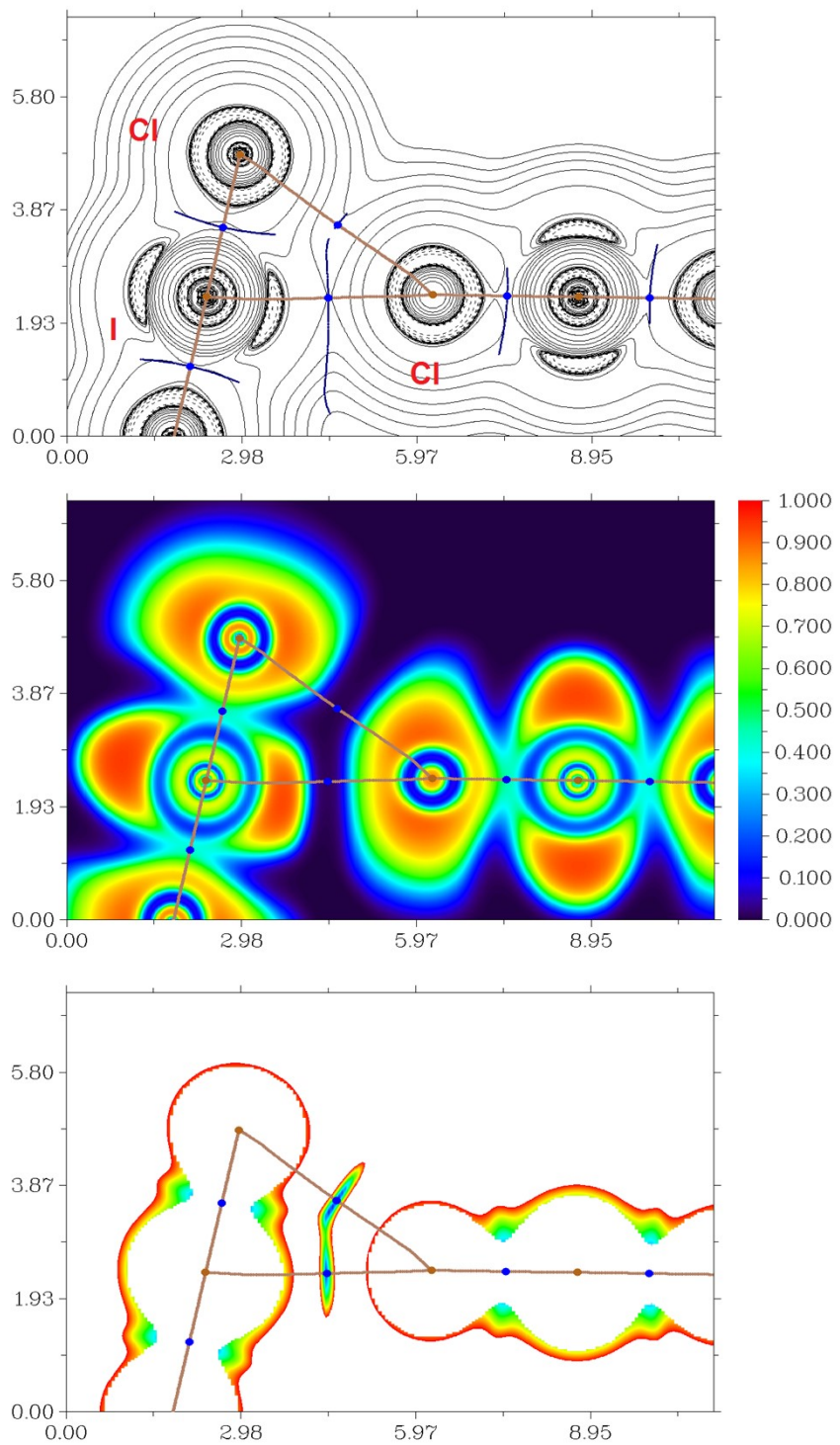


**Figure S9.** Contour line diagram of the Laplacian of electron density distribution  $\nabla^2\rho(\mathbf{r})$ , bond paths, and selected zero-flux surfaces (top), visualization of electron localization function (ELF, center) and reduced density gradient (RDG, bottom) analyses for intermolecular interactions Cl...Cl and Cl...I in **4**. Bond critical points (3, -1) are shown in blue, nuclear critical points (3, -3) – in pale brown, bond paths are shown as pale brown lines, length units – Å, and the color scale for the ELF and RDG maps is presented in a.u.

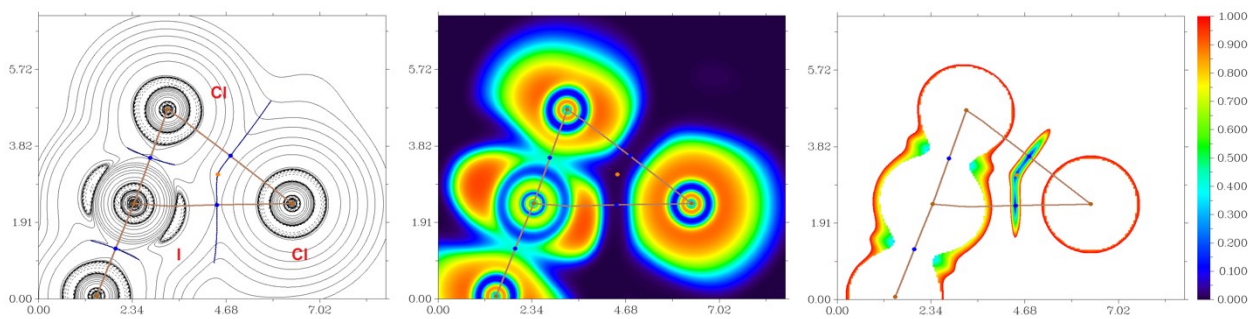


**Figure S10.** Contour line diagram of the Laplacian of electron density distribution  $\nabla^2\rho(\mathbf{r})$ , bond paths, and selected zero-flux surfaces (left), visualization of electron localization function (ELF, center) and reduced density gradient (RDG, right) analyses for intermolecular interactions  $\text{Cl}\cdots\text{Cl}$  and  $\text{Cl}\cdots\text{I}$  (3.887 and 3.943 Å, respectively) in **5**. Bond critical points (3, -1) are shown in blue, nuclear critical points (3, -3) – in pale brown, ring critical points (3, +1) – in orange, bond paths are shown as pale brown lines, length units – Å, and the color scale for the ELF and RDG maps is presented in a.u.

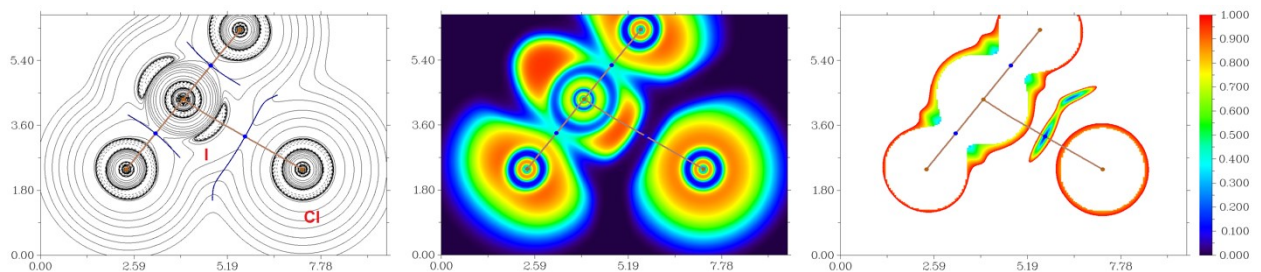


**Figure S11.** Contour line diagram of the Laplacian of electron density distribution  $\nabla^2\rho(\mathbf{r})$ , bond paths, and selected zero-flux surfaces (left), visualization of electron localization function (ELF, center) and reduced density gradient (RDG, right) analyses for intermolecular interactions  $\text{Cl}\cdots\text{I}$  in **7**. Bond critical points (3, -1) are shown in blue, nuclear critical points (3, -3) – in pale brown, bond paths are shown as pale brown lines, length units – Å, and the color scale for the ELF and RDG maps is presented in a.u.

The balance between the Lagrangian kinetic energy  $G(\mathbf{r})$  and potential energy density  $V(\mathbf{r})$  at the bond critical points (3, -1) reveals the nature of these interactions, if the ratio  $-G(\mathbf{r})/V(\mathbf{r}) > 1$  is satisfied, than the nature of appropriate interaction is purely non-covalent, in case the  $-G(\mathbf{r})/V(\mathbf{r}) < 1$  some covalent component takes place [J. Chem. Phys. 2002, 117, 5529.]; based on this criterion one can state that a covalent contribution in intermolecular interactions  $\text{Cl}\cdots\text{Cl}$  and  $\text{Cl}\cdots\text{I}$  in the X-ray structures **1–9** is absent (**Table S4**). The Laplacian of electron density is typically decomposed into the sum of contributions along the three principal axes of maximal variation, giving the three eigenvalues of the Hessian matrix ( $\lambda_1$ ,  $\lambda_2$  and  $\lambda_3$ ), and the sign of  $\lambda_2$  can be utilized to distinguish bonding (attractive,  $\lambda_2 < 0$ ) weak interactions from non-bonding ones (repulsive,  $\lambda_2 > 0$ ).[J. Am. Chem. Soc. 2010, 132, 6498. || J. Chem. Theory Comput. 2011, 7, 625.] Thus, all discussed intermolecular interactions  $\text{Cl}\cdots\text{Cl}$  and  $\text{Cl}\cdots\text{I}$  in the X-ray structures **1–9** are attractive.

## Computational details

The DFT calculations based on the experimental X-ray geometries of **1–9** have been carried out using the dispersion-corrected hybrid functional wB97XD [Phys. Chem. Chem. Phys. 2008, 10, 6615.] with the help of Gaussian-09 [M. J. Frisch, G. W. Trucks, H. B. Schlegel, G. E. Scuseria, M. A. Robb, J. R. Cheeseman, G. Scalmani, V. Barone, B. Mennucci, G. A. Petersson, H. Nakatsuji, M. Caricato, X. Li, H. P. Hratchian, A. F. Izmaylov, J. Bloino, G. Zheng, J. L. Sonnenberg, M. Hada, M. Ehara, K. Toyota, R. Fukuda, J. Hasegawa, M. Ishida, T. Nakajima, Y. Honda, O. Kitao, H. Nakai, T. Vreven, M. J. A.; J. E. Peralta, F. Ogliaro, M. Bearpark, J. J. Heyd, E. Brothers, K. N. Kudin, V. N. Staroverov, T. Keith, R. Kobayashi, J. Normand, K. Raghavachari, A. Rendell, J. C. Burant, S. S. Iyengar, J. Tomasi, M. Cossi, N. Rega, J. M. Millam, M. Klene, J. E. Knox, J. B. Cross, V. Bakken, C. Adamo, J. Jaramillo, R. Gomperts, R. E. Stratmann, O. Yazyev, A. J. Austin, R. Cammi, C. Pomelli, J. W. Ochterski, R. L. Martin, K. Morokuma, V. G. Zakrzewski, G. A. Voth, P. Salvador, J. J. Dannenberg, S. Dapprich, A. D. Daniels, O. Farkas, J. B. Foresman, J. V. Ortiz, C. J.; D. J. Fox, in Gaussian 09, Revision C.01, Gaussian, Inc., Wallingford, CT, 2010.] program package. The Douglas–Kroll–Hess 2<sup>nd</sup> order scalar relativistic calculations requested relativistic core Hamiltonian were carried out using the DZP-DKH basis sets [Mol. Phys. 2010, 108, 1965. || J. Chem. Phys. 2009, 130, 064108. || Chem. Phys. Lett. 2013, 582, 158. || J. Mol. Struct. - Theochem 2010, 961, 107.] for all atoms. The topological analysis of the electron density distribution in model supramolecular associates **1–9** and calculation of molecular surface electrostatic potential distribution on the optimized equilibrium model structure  $[\text{ICl}_4]^-$  have been performed by using the Multiwfn program (version 3.7) [J. Comput. Chem. 2012, 33, 580.]. The Chemcraft program [<http://www.chemcraftprog.com/>] was used for the visualization. The Cartesian atomic coordinates for model supramolecular associates **1–9** and optimized equilibrium model structure  $[\text{ICl}_4]^-$  presented in **Table S5**.

**Table S6.** Cartesian atomic coordinates for model structures.

Atom	X	Y	Z
<b>1</b>			
I	6.759102	4.925000	7.506745
Cl	4.317899	4.787002	7.054088
Cl	7.127966	2.969578	6.014404
Cl	9.200304	5.062999	7.959401
Cl	6.390238	6.880422	8.999086
I	-1.558398	4.925000	7.506745
Cl	-3.999601	4.787002	7.054088
Cl	-1.189534	2.969578	6.014404
Cl	0.882804	5.062999	7.959401
Cl	-1.927262	6.880422	8.999086
I	7.538301	9.850000	3.753372
Cl	9.979503	9.712001	4.206029
Cl	7.169437	7.894578	5.245713
Cl	5.097098	9.987998	3.300716
Cl	7.907165	11.805422	2.261032
<b>2</b>			
I	1.568569	5.915150	11.828130

Cl	2.419195	5.034148	9.653055
Cl	0.605015	7.907964	10.649457
Cl	0.717943	6.796152	14.003205
Cl	2.532123	3.922336	13.006803
I	-2.802131	5.915150	11.828130
Cl	-1.951505	5.034148	9.653055
Cl	-3.765685	7.907964	10.649457
Cl	-3.652757	6.796152	14.003205
Cl	-1.838577	3.922336	13.006803
I	1.876960	0.000000	5.914065
Cl	1.026334	-0.881002	8.089140
Cl	2.840514	1.992814	7.092738
Cl	2.727585	0.881002	3.738990
Cl	0.913405	-1.992814	4.735392
<b>3</b>			
I	3.060964	7.272082	2.122558
Cl	5.437833	7.517423	2.719654
Cl	0.629423	6.958864	1.498759
Cl	2.780748	5.601426	3.960954
Cl	3.359066	9.004436	0.347290
Cl	5.434770	3.870230	3.069415
N	8.836492	2.546103	1.633227
C	7.864518	3.369700	2.067638
H	7.998567	4.310425	2.089901
C	6.669173	2.817417	2.479731
C	6.463466	1.471468	2.441471
H	5.633170	1.102288	2.718881
C	7.484875	0.650767	1.991915
H	7.364383	-0.291107	1.954620
C	8.677009	1.215602	1.599750
H	9.389494	0.661446	1.303361
C	10.157376	3.139904	1.160556
H	10.849279	2.976719	1.835671
H	10.052523	4.105240	1.027785
H	10.420575	2.720332	0.315295
I	2.874835	2.444432	5.848292
Cl	0.497966	2.689773	5.251196
Cl	5.306376	2.131214	6.472091
Cl	3.155051	0.773776	4.009895
Cl	2.576733	4.176786	7.623560
I	11.265364	7.272082	2.122558
Cl	13.642233	7.517423	2.719654
Cl	8.833823	6.958864	1.498759
Cl	10.985148	5.601426	3.960954
Cl	11.563466	9.004436	0.347290
<b>4</b>			
Cl	5.937412	7.892343	4.243155
I	3.505644	7.478625	3.830668
Cl	2.955179	9.425860	5.299653
Cl	1.073876	7.064907	3.418182
Cl	4.056109	5.531390	2.361684
Cl	1.930132	2.906593	-0.412486

I	4.361900	2.492875	0.000000
Cl	4.912365	4.440110	-1.468985
Cl	6.793668	2.079157	0.412486
Cl	3.811435	0.545640	1.468985
<b>5</b>			
Cl	4.345836	11.145515	9.465550
Cl	2.011164	8.484193	9.433640
I	4.360513	8.782269	8.671897
Cl	4.385629	6.397233	7.974968
Cl	6.721591	9.067237	7.896397
Cl	1.715289	5.877685	4.716962
Cl	4.049961	8.539007	4.748872
I	1.700612	8.240931	5.510615
Cl	1.675497	10.625967	6.207544
Cl	-0.660465	7.955963	6.286115
<b>6</b>			
I	4.179416	10.434518	6.822547
Cl	4.048244	10.693037	9.305700
Cl	4.379302	10.138339	4.363228
Cl	6.130652	8.888037	7.168219
Cl	2.271981	12.010432	6.457643
I	4.640718	9.973216	-1.396003
Cl	4.899237	9.842044	1.087150
Cl	4.344539	10.173102	-3.855322
Cl	3.094237	11.924452	-1.050331
Cl	6.216632	8.065781	-1.760907
I	7.408184	12.740682	6.822547
Cl	7.539356	12.482163	9.305700
Cl	7.208298	13.036861	4.363228
Cl	5.456948	14.287163	7.168219
Cl	9.315619	11.164768	6.457643
<b>7</b>			
I	0.943427	-0.698852	7.513939
Cl	2.940825	-0.912247	8.996965
Cl	2.393191	-0.239379	5.542206
Cl	-1.053971	-0.485456	6.030913
Cl	-0.506337	-1.158324	9.485671
Cl	0.605070	3.124004	7.513939
I	-1.857496	-1.397703	15.027878
Cl	0.139902	-1.611099	16.510904
Cl	-0.407733	-0.938231	13.056145
Cl	-3.854894	-1.184308	13.544851
Cl	-3.307260	-1.857176	16.999610
<b>8</b>			
I	-0.333477	7.234444	7.169818
Cl	0.606038	9.517686	7.447280
Cl	0.866367	6.940237	4.981467
Cl	-1.273681	4.910207	7.035284
Cl	-1.541963	7.542638	9.323207
I	-2.258010	8.842456	3.456857
Cl	-3.197525	6.559214	3.179395
Cl	-3.457853	9.136663	5.645209

Cl	-1.317806	11.166693	3.591391
Cl	-1.049524	8.534262	1.303468
I	-4.849496	8.842456	14.083533
Cl	-5.789012	6.559214	13.806070
Cl	-6.049340	9.136663	16.271884
Cl	-3.909293	11.166693	14.218067
Cl	-3.641011	8.534262	11.930143
<b>9</b>			
I	2.242214	11.221631	10.557647
Cl	1.292558	12.964404	12.090604
Cl	3.203045	9.581333	9.015305
Cl	3.115943	12.960134	9.026750
Cl	1.421567	9.347920	11.993320
I	5.558409	5.530188	6.124731
Cl	6.715055	3.851320	4.646711
Cl	4.493138	7.187423	7.570934
Cl	6.740528	7.371023	4.967173
Cl	4.298391	3.733190	7.332876
I	6.063681	15.989526	5.270354
Cl	7.185898	17.561508	3.705923
Cl	5.249937	17.894549	6.612979
Cl	4.946724	14.471628	6.872783
Cl	6.831739	14.021880	3.960005
I	7.772273	11.489060	1.455321
Cl	5.849789	11.674937	-0.109110
Cl	6.529347	9.831826	2.797945
Cl	9.645291	11.280696	3.057749
Cl	9.092276	13.138040	0.144971
I	8.597111	20.912413	2.927580
Cl	10.581224	20.863453	4.460537
Cl	6.696156	20.900458	1.385239
Cl	9.665834	19.286490	1.396684
Cl	7.384753	22.559970	4.363254
I	0.648662	16.281150	13.754797
Cl	1.524281	18.122269	12.276777
Cl	-0.253910	14.529981	15.201000
Cl	-1.536607	16.384479	12.597240
Cl	2.834917	16.088442	14.962942
I	0.379961	6.679892	14.372680
Cl	2.364074	6.630932	15.905637
Cl	-1.520994	6.667936	12.830339
Cl	1.448684	5.053968	12.841784
Cl	-0.832397	8.327448	15.808354
I	2.598345	0.986456	9.085387
Cl	3.398613	-0.771403	7.520957
Cl	4.655015	0.738668	10.428012
Cl	1.842285	2.712719	10.687816
Cl	0.510285	1.305122	7.775038
I	8.865812	2.048629	2.309697
Cl	9.741431	3.889748	0.831677
Cl	7.963240	0.297460	3.755900
Cl	6.680543	2.151957	1.152140

Cl	11.052067	1.855921	3.517842
$[\text{ICl}_4]^-$			
I	1.568569	5.915150	11.828130
Cl	2.444626	5.010503	9.578165
Cl	0.579753	7.962589	10.609849
Cl	0.692513	6.819797	14.078096
Cl	2.557385	3.867711	13.046411

The Hirshfeld surfaces analysis was performed in CrystalExplorer program (version 17.5) [M. J. Turner, J. J. McKinnon, S. K. Wolff, D. J. Grimwood, P. R. Spackman, D. Jayatilaka and M. A. Spackman, CrystalExplorer17 (2017). University of Western Australia. <http://hirshfeldsurface.net> || CrystEngComm 2009, 11, 19.]]. The normalized contact distances ( $d_{\text{norm}}$  [Chem. Commun. 2007, 3814.]) based on Bondi's van der Waals radii [J. Phys. Chem. 1966, 70, 3006.] were mapped into the Hirshfeld surfaces.

**Table S7.** Partial contributions of different interatomic contacts to the Hirshfeld surfaces of the  $\{\text{ICl}_4\}$  moieties in the X-ray structures **1–9**.

X-ray structure	Contributions of different interatomic contacts to the Hirshfeld surfaces
<b>1</b>	Cl–H 81.3%, I–Cl 5.8%, I–H 4.7%, Cl–C 4.7%, Cl–Cl 2.1%, Cl–N 1.3%
<b>2</b>	Cl–H 79.4%, I–Cl 7.0%, Cl–Cl 5.8%, I–H 3.2%, Cl–C 3.1%, I–I 1.1%, Cl–N 0.4%
<b>3</b>	Cl–H 61.7%, Cl–Cl 15.2%, Cl–C 10.5%, I–Cl 7.2%, I–H 3.1%, Cl–N 2.1%, I–C 0.2%
<b>4</b>	Cl–H 80.6%, I–Cl 5.9%, I–H 4.7%, Cl–C 4.3%, Cl–Cl 2.6%, Cl–N 2.0%
<b>5</b>	Cl–H 83.0%, I–Cl 4.7%, I–C 3.3%, Cl–Cl 3.2%, Cl–C 2.5%, I–H 1.3%, Cl–N 1.0%, I–I .7%, I–N 0.2%
<b>6</b>	Cl–H 67.1%, Cl–Cl 14.0%, Cl–C 6.7%, I–Cl 4.8%, I–H 3.2%, I–I 2.2%, Cl–N 2.1%
<b>7</b>	Cl–H 87.5%, I–H 4.8%, I–Cl 3.4%, Cl–Cl 2.5%, Cl–C 1.8%
<b>8</b>	Cl–H 82.3%, I–Cl 4.8%, Cl–Cl 3.9%, Cl–C 3.8%, I–C 3.8%, I–H 0.8%, I–I 0.5%
<b>9</b>	Cl–H 81.2%, Cl–Cl 8.0%, I–Cl 7.0%, I–H 3.8%